Design and Expression of Cysteine-Bearing Hydrophobic Polypeptides and Their Self-Assembling Properties with Bacteriochlorophyll *a* Derivatives as a Mimic of Bacterial Photosynthetic Antenna Complexes. Effect of Steric Confinement and Orientation of the Polypeptides on the Pigment/Polypeptide Assembly Process†

Takehisa Dewa,*,‡,§ Taku Yamada,‡ Makiko Ogawa,‡ Miku Sugimoto,‡ Taeko Mizuno,‡ Kiyotaka Yoshida,‡ Yoshiaki Nakao,‡ Masaharu Kondo,‡ Kouji Iida,|| Keiji Yamashita,‡ Toshiki Tanaka,‡ and Mamoru Nango*,‡

Materials Science and Engineering, Nagoya Institute of Technology, Gokiso-cho, Showa-ku, Nagoya 466-8555, Japan, PRESTO, JST, and Nagoya Municipal Industrial Research Institute, 3-4-41 Rokuban-cho, Atsuta-ku, Nagoya 456-0058, Japan

Received October 6, 2004; Revised Manuscript Received December 8, 2004

ABSTRACT: A series of cysteine-bearing hydrophobic polypeptides analogous to a light-harvesting one β polypeptide (LH1β) from the LH1 complex from the purple photosynthetic bacterium, *Rhodobacter sphaeroides*, was synthesized using an *Escherichia coli* expression system. The cysteine was placed in the C- or N-terminal regions of the polypeptide to investigate the influence of steric confinement and orientation of the polypeptides via disulfide linkages as they were self-assembled with zinc-substituted bacteriochlorophyll *a* ([Zn]-BChl *a*). The polypeptides were expressed as water-soluble fusion proteins with maltose-binding protein (MBP). The fusion proteins formed a subunit-type complex with the [Zn]-BChl *a* in an *n*-octyl-β-D-glucopyranoside (OG) micellar solution regardless of the cross-links or the cleavage of the cysteines, judging from absorption, CD, and fluorescence spectra. Following treatment with trypsin, the polypeptides were detached from the MBP portion. Such trypsin-digested polypeptides formed a subunit-type LH complex at 25 °C, which also showed that the disulfide linkage was not crucial for the subunit formation. When a polypeptide having cysteine on the C-terminus was assembled at 4 °C, the Qy absorption band was remarkably red-shifted to ∼836 nm, suggesting that the cleavage of the large MBP portion liberates the polypeptides to form the progressive type of complex similar to LH1-type complex. The trypsin-treated polypeptides bearing cysteines in both terminal regions, which are randomly cross-linked, did not form the LH1-type complex under oxidative conditions but did form the complex under reductive conditions. This observation suggests that the polypeptide orientation strongly influences the LH1-type complex formation. The progressive assembly from the subunit to the holo-LH1-type complex following cleavage of MBP portion in a lipid bilayer is also briefly discussed.

In the primary photosynthetic event, pigment/transmembrane protein complexes, that is, light-harvesting (LH)[1] complexes and photosynthetic reaction centers (RC), cooperate to efficiently transduce light energy (*1*−*3*). Recently, X-ray crystallography has successfully revealed the structures of these important components in a photosynthetic apparatus (*4*−*7*), and their structure and function are now quite well understood. In the primary process, a photon is captured by peripheral antenna complex, LH2 (*4*), funneled into a core antenna, LH1, and subsequently transferred to an RC (*5*, *6*) where charge separation takes place. The two types of antenna complex, LH1 and LH2, consist of essentially similar "building blocks", that is, pigments, bacteriochlorophyll *a* (BChl *a*), and carotenoids, and two apoproteins, LHα and LHβ, both of which are α-helical transmembrane polypeptides (M_w ∼ 6 kDa). The high-resolution X-ray crystallography has revealed the structure of LH2 complexes: an oligomeric annular structure composed of α,β-heterodimers as a minimum unit. For the LH1 complex, an electron microscopic projection map of the two-dimensional crystal had suggested that the structure is a larger ring that is big enough to surround a centrally located RC (*8*). Recently, a 3D crystallographic structure of the RC-LH1 core complex of *Rhodopseudomonas palustris* at 4.8 Å resolution has been

† This work is supported by PRESTO (Japan Science and Technology Agency), a Grant-in-Aid for Scientific Research on Priority Areas (417) from the Ministry of Education, Culture, Sports, Science, and Technology, NEDO International Joint Grant, Japan, and also NITECH 21st Century COE Program "World Ceramics Center for Environmental Harmony".

* To whom correspondence should be addressed. Tel/fax: +81−52−735−5226; e-mail: nango@nitech.ac.jp.

‡ Nagoya Institute of Technology.

§ PRESTO, JST.

|| Nagoya Municipal Industrial Research Institute.

[1] Abbreviations: LH1, the core light-harvesting complex; LH2, the peripheral light-harvesting complex; RC, photosynthetic reaction center; OG, *n*-octyl β-D-glucopyranoside; MBP, maltose-binding protein; BChl *a*, bacteriochlorophyll *a*; [Zn]-BChl *a*, zinc-substituted bacteriochlorophyll *a* also termed zinc-bacteriopheophytin; SDS, sodium dodecyl sulfate; PAGE, polyacrylamide gel electrophoresis; NIR, near-infrared; CD, circular dichroism; RP-HPLC, reverse-phase high-performance liquid chromatography; DOPG, 1,2-dioleoylphosphatidylglycerol. The following abbreviations were used to refer to the series of MBP-fusion protein attaching polypeptides **1**−**4**: MBP-**1**−**4**, and their corresponding cross-linked forms, (MBP-**2**)$_2$, (MBP-**3**)$_2$, and (MBP-**4**)$_n$.

10.1021/bi0478493 CCC: $30.25
Published on Web 03/09/2005

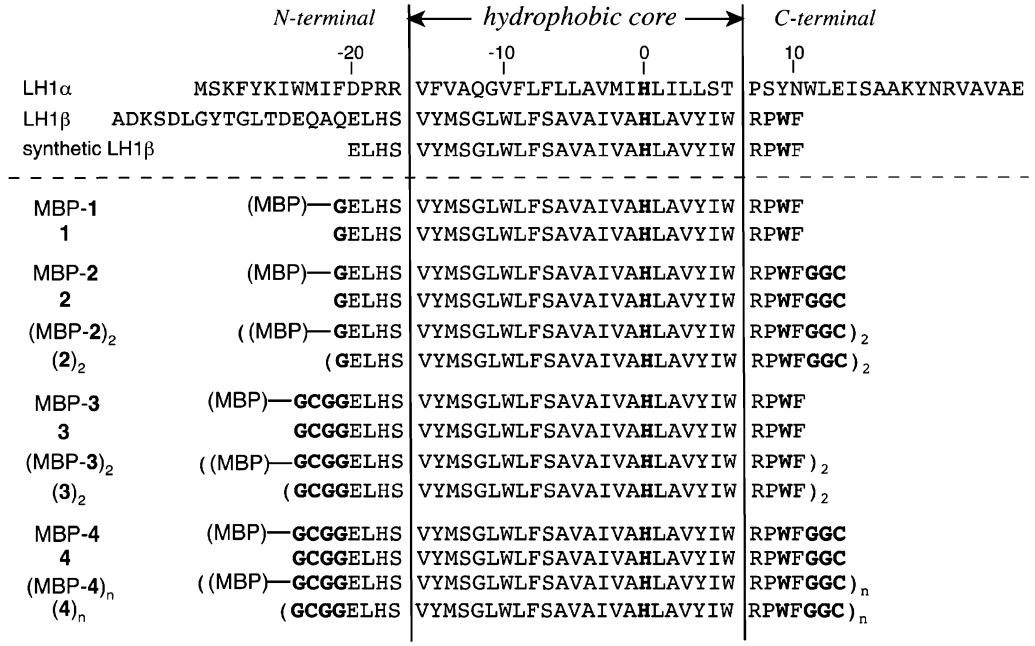

FIGURE 1: Amino acid sequences of LH1α and *β* of *Rhodobacter sphaeroides*, chemically synthesized LH1*β*, MBP-fused polypeptides, MBP-**1**−MBP-**4**, enzymatically cleaved polypeptides, **1**−**4**, and their corresponding oxidized forms, (MBP-**2**)$_2$, (MBP-**3**)$_2$, (MBP-**4**)$_n$, (**2**)$_2$, (**3**)$_2$, and (**4**)$_n$ studied in this paper. The position 0 represents the His to which pigments BChl *a* and [Zn]-BChl *a* are coordinated.

reported (*7*). The structure indicates that the RC is surrounded by the ellipsoidal 15-membered LH1 complex together with an additional transmembrane polypeptide, which is assumed to play an important role of a portal for the secondary electron acceptor ubiquinone. Structural analysis by using atomic force microscopy (AFM) also has shown an elliptical RC-LH1 complex of *Rhodospirillum (Rs.) rubrum* (*9*). Meanwhile, AFM images of LH1 complex of *Rhodobacter (Rb.) sphaeroides* have suggested the structural flexibility and the size heterogeneity (*10*). A very recent report has exhibited AFM images of multicomponents comprising LH2 and RC-LH1: these are divided into specialized domains (*11*, *12*). However, how these components as functional supramolecular assemblies are organized in the photosynthetic membrane still remains to be clarified.

The BChls and the LH polypeptides assemble to form LH complex, where the BChls (B870 in LH1 and B850 in LH2) are precisely aligned to produce an excitonically coupled array. For the LH1 complex, Miller et al. have found that these building blocks, separately isolated from photosynthetic bacteria, can be reconstituted in an *n*-octyl *β*-D-glucopyranoside (OG) micellar solution and that the reconstituted complex spectroscopically resembles intact bacterial LH1 complex (*13*). They have also described the structural intermediate of LH1, the so-called subunit-type complex (B820), consisting of an α/*β* heterodimer (α/*β*/BChl *a* = 1/1/2 in the stoichiometry), and how this depends on the OG concentration and the temperature. The essential amino acids in the LH1*β* polypeptide for subunit- or LH1-type complex formation are H (0) and W (+9) for coordination to magnesium and hydrogen bonds to a carbonyl group of BChl *a*, respectively (*14*, *15*). (The numbering of amino acid is described in Figure 1.) Amino acids at the position +4 (Y), +6 (W), and +7 (R) of the *β* polypeptide, which are also highly conserved in many species of purple bacteria, contribute important stabilizing interactions in the B820 subunit and LH1 complexes (*16*−*18*).

The structure of subunit-type complex as the minimal unit of LH1 complexes has been well studied recently using multidimensional NMR spectroscopy and small-angle neutron scattering (*19*−*22*). The LH1*β* polypeptide of *Rb. sphaeroides* can form a subunit-type complex with BChl *a* in the absence of LH1α polypeptide. In addition, the LH1*β* polypeptide is of particular interest because it assembles on the outside of the complex and, therefore, may interact with LH2. A recent study has suggested that the N-terminal domain of the LH1*β* is likely to point toward the center of the LH1 complex, implying that the N-terminal domain may interact with not only LH1α but also the RC (*19*). Meanwhile, it has been reported that a synthetic LH1*β* polypeptide lacking the N-terminal region rich in charged amino acids associates with BChl *a* or zinc-substituted bacteriochlorophyll *a* ([Zn]-BChl *a*) to form an LH1-type complex (*16*, *23*−*26*). (The sequence is shown in Figure 1 as "synthetic LH1*β*".) The α-helical LH polypeptides in both subunit- and LH1-type complexes assemble with the pigments aligned in the same direction. In photosynthetic membranes, in fact, the C- and N-termini of the LH polypeptides are found on the periplasmic and cytoplasmic sides, respectively.

These orientationally regulated self-assembling properties of these pigment/polypeptide combinations are particularly intriguing. What essential interactions, such as protein−protein and protein−pigment interactions, control this process (*27*)? An understanding of the answer to this question will be very useful in the design and construction of artificial energy-conversion systems (*28*, *29*) and biomolecular devices, for example, for use as photosensitizers and in nonlinear optical devices. Various de novo designed helical bundles to mimic redox enzymes have been reported (*30*−*33*). Our alternative approach is to make use of the self-assembly properties to produce a similar biomimetic structure using BChls rather than porphyrins. Recently, we have reported self-assembling properties of pigments, BChl

Scheme 1: Gene Sequences of the Polypeptides **1**−**4**

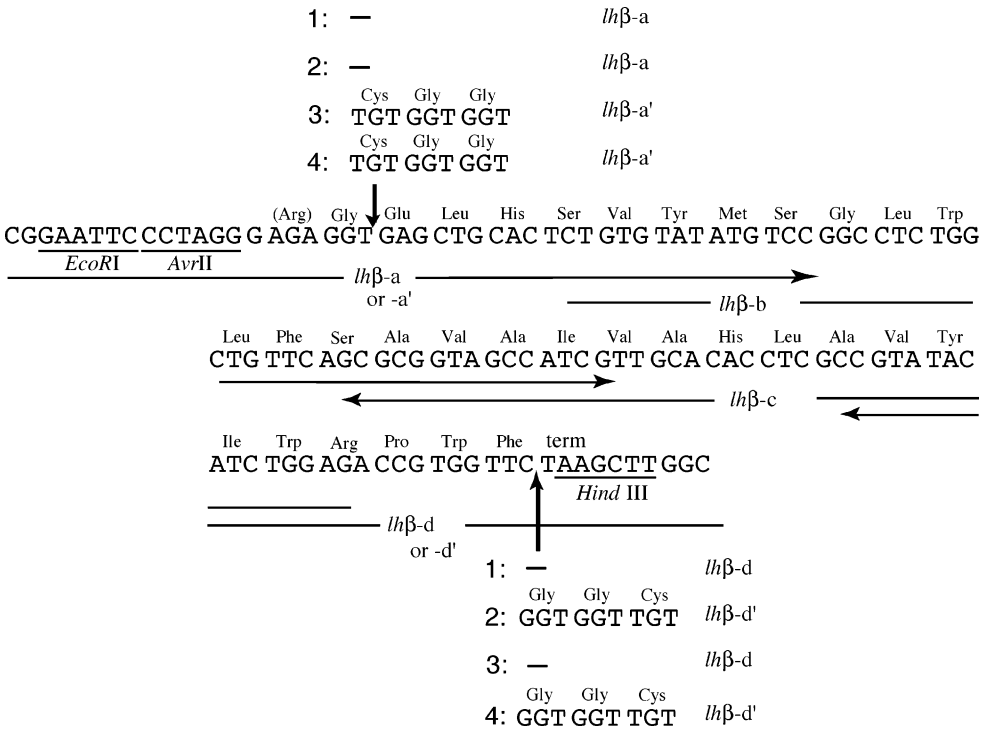

a and [Zn]-BChl *a*, with a series of chemically synthesized LH1-model polypeptides (*24*−*26*, *34*).

There are many examples of using hydrophobic polypeptides as a mimic of LH polypeptides where they have been made by chemical synthesis (*16*, *24*−*26*, *34*) or genetic manipulation in photosynthetic bacteria (*35*), however, little has been paid to use *Escherichia coli* expression systems. The highly hydrophobic property of these polypeptides might be thought to be inappropriate because of their toxicity for *E. coli*. However, an *E. coli* expression system where such toxicity could be avoided could be a potential candidate for the production of a wide variety of the mutated LH polypeptides. The key to successful overexpression would be choosing an appropriate tag that provides enough solubility for the hydrophobic portion to avoid formation of inclusion bodies. We, therefore, chose a maltose-binding protein (MBP) as the tag (whose molecular weight is ∼40 kDa).

In this report, we describe (i) the first example of successful overexpression of LH polypeptides as MBP-fusion proteins and (ii) the effects of the steric confinement and the orientation of polypeptides on their self-assembling properties. We have assessed the essential structural factors for the formation of the subunit and the LH1-type complexes. We designed polypeptides bearing cysteines of the C- or N-terminal regions, **2**−**4** (Figure 1). The amino acid sequence of the hydrophobic core region was identical with LH1β polypeptide of *Rb. sphaeroides*. The orientation of the polypeptides are controllable via the redox state of the cysteines: the oxidized forms, $(\mathbf{2})_2$ and $(\mathbf{3})_2$, are cross-linked at N- and C-terminal regions, respectively, and $(\mathbf{4})_n$ is randomly cross-linked, while the reduced forms, **2**−**4**, are free from such confinements. The polypeptide **1** lacking cysteine was used as a reference polypeptide. Transformation of the subunit-type complex into the holo-LH1-complex following MBP-cleavage in a lipid bilayer is also briefly discussed.

EXPERIMENTAL PROCEDURES

Materials. Unless stated otherwise, all chemicals and reagents were obtained commercially and used without further purification. A BChl *a* bearing geranylgeraniol ester side chain was isolated from carotenoidless mutant G9 of *Rs. rubrum* and purified by HPLC as described elsewhere (*18*). A [Zn]-BChl *a* was prepared from BChl *a* via transmetalation by following a procedure previously reported (*23*, *34*).

*Bacterial Expression of LH Model Polypeptides as MBP-Fusion Proteins, MBP-**1**, -**2**, -**3**, and -**4***. The hydrophobic polypeptides, **1**−**4**, were obtained as C-terminal fusions with MBP (*36*). The commercially available vector, pMal-c2 (New England Biolabs), codes a linker sequence, ISEF, between Factor Xa site, IEGR, and a start cloning site. Hydrolysis by Factor Xa will leave the extra sequence, ISEF, on the motive polypeptides. To avoid the influence of the ISEF portion upon the assembly properties of the designed polypeptides, we modified the vector so as not to contain the unnecessary linker site. The modification of the vector was at first carried out by introduction of another restriction site, *Avr*II, on the upstream of the IEGR site as described below. The small fragment between the *Nco*I−*Bam*HI sites on the vector was amplified by PCR using the primers, 5′ GCCACCATGGAAAACGCCCAG 3′ (Mal-*Nco*: the underlined part is *Nco*I site) and 5′ CG**GGATCC**TGAATTC-CTTCCCTCGATCCCTAGGTTGTTGTTATTG 3′ (Mal-*Avr*: the bold and the underlined parts are *Bam*HI and *Avr*II sites, respectively). The amplified DNA was inserted into a large fragment of *Nco*I−*Bam*HI site of a pMal-c2 vector.

Scheme 1 shows the gene sequences coding polypeptides **1**−**4**. Three of the restriction enzyme sites, *Eco*RI, *Avr*II,

and *Hind*III, were attached on the up- (for *Eco*RI and *Avr*II) and downstream (for *Hind*III) of the sequences. A codon for arginine, AGA, was inserted after the *Avr*II site on the *lhβ*-a (-a′) so as to be able to enzymatically release the polypeptide from the MBP tag. The *lhβ*-a (or -a′), -b, -c, and -d (or -d′) were subjected to PCR for 26 cycles to obtain the gene for the polypeptides, **1**−**4**. The PCR product was isolated by electrophoresis in 10% agarose gels, followed by precipitation with ethanol. The purified product was treated with *Eco*RI and *Hind*III and then ligated into the large fragment of an *Eco*RI−*Hind*III site of pUC119 (Pharmacia). The nucleotide sequences were confirmed by DNA sequencing. The recovered plasmid was treated with *Avr*II and *Hind*III, and then the resulting small fragment was ligated into the large fragment of an *Avr*II−*Hind*III site of the premodified pMAL-c2 vector.

The resulting plasmid was introduced into *E. coli*, JM109, by heat shock at 37 °C for 30 s. The transfected *E. coli* was cultured in an LB medium containing ampicillin at 37 °C overnight. The overnight culture (12 mL) was transferred into a large-scaled medium (1 L) and grown for 3 h at 37 °C. Then, 1 mM isopropyl-1-thio-*β*-D-galactopyranoside (IPTG) was added to induce the expression. After 4 h, the cells were harvested (wet volume: ca. 1.5 mL) and suspended in 15 mL of solution A (20 mM Tris-HCl (pH 7.5), 0.2 M NaCl, 1 mM EDTA, 1 mM NaN_3), followed by sonication in an ice bath. The homogenized cell solution was centrifuged at 14 000*g* for 20 min at 4 °C. The supernatant was collected and applied to an amylose resin column (6 mL) (New England Biolabs) at 4 °C, which was preequilibrated in solution A. After washing with the solution A, the fusion protein was eluted with the solution A containing 20 mM maltose. The concentration of MBP-fusion proteins (MBP-**1**, -**2**, -**3**, and -**4**) was determined by the extinction coefficient ($E_M^{280} = 87\,430\ M^{-1}\ cm^{-1}$) calculated from the number of tyrosine ($E_M^{280} = 1390\ M^{-1}\ cm^{-1}$) and tryptophan ($E_M^{280} = 5800\ M^{-1}\ cm^{-1}$) in water (*37*). The fusion protein was then treated with trypsin (final 0.55 *μ*M) at 37 °C for 24 h. The reaction was stopped by adding leupeptin (0.64 *μ*M) and aprotinin (5 *μ*g/mL) and stood for 1 h. The correct hydrolysis was confirmed by SDS−PAGE and reverse-phase (RP) HPLC.

Polypeptide Analysis and Purification. The affinity-chromatographed fusion protein and the hydrolyzed crude mixture were analyzed by using high-performance liquid chromatograph (Shimazu LC-VP series) equipped with a reverse-phase column (YMC-Pack Protein-RP: 250 × 4.6 mm, 5 *μ*m). A sample was eluted with linear gradient of an organic solution (acetonitrile/2-propanol (1/1, v/v) containing 0.1% TFA) and 0.1% TFA of an aqueous solution at a flow rate of 0.8 mL/min. The fraction containing LH polypeptide was pooled and lyophilized. Mass spectral analysis (MALDI-TOF-MS) for polypeptide **2**, for instance, exhibited a single peak at 4032.90 (*m*/*z*), which is in good agreement with the expected mass (4032.68 *m*/*z*).

Reconstitution Assay. Assembly of pigment/polypeptide mixture was carried out using the method which has been established for the reconstitution of native LH polypeptide with BChl *a* in an *n*-octyl-*β*-D-glucopyranoside (OG) micellar solution (*18*, *38*). The pigments, BChl *a* and [Zn]-BChl *a*, were handled in a dark room to prevent photodegradation. In a typical experiment, OG of 0.9 wt % of concentration was added to a solution A (1.3 mL) containing 10 nmol of the fusion protein or the enzymatically cleaved polypeptide. Then, 5 nmol of pigment (BChl *a* or [Zn]-BChl *a*) was added as a degassed acetone solution, followed by dilution of this mixture with 0.2 mL of solution A (down to 0.78 wt % of the final OG concentration). The solution was cooled at 4 °C for 3 days and then was subjected to spectroscopic measurements. The redox state of the cysteine residues was controlled by the presence or absence of 2-mercaptoethanol (1 *μ*L). Incorporation of a reconstituted product into a lipid bilayer was carried out by the following procedure. To a reconstituted sample solution, 100 nmol of 1,2-dioleoylphosphatidylglycerol (DOPG: Nippon Fine Chemical Co., Ltd., Japan) dissolved in Solution A containing 0.78 wt % OG was added. The resulting solution was subjected to dialysis against phosphate buffer solution (50 mM, pH 7.0) for 30 h.

Near-infrared absorption (HITACHI U-2000 spectrophotometer) and circular dichroism (Jasco J-600 or J-820 spectropolarimeter) spectroscopy was conducted to observe pigment/polypeptide assemblies. Steady-state fluorescence spectra were obtained using a spectrometer composed of a CCD detector (Spec-10: 100BR/LN; Roper Scientific), monochromators (SP-150M for excitation and SP-306 for emission; Acton Research Co.), and a lamp house (tungsten−halogen light source, TS-428DC; Acton Research Co.). All the spectroscopic measurements used sample solutions that were placed in a temperature-controlled chamber.

RESULTS

Bacterial Expression of the Fusion Proteins and the Hydrolytic Cleavage. Initially, we tried a direct expression of these hydrophobic polypeptides alone. However, this was unsuccessful. It has been reported that pMal-c2 vector is suitable for an overexpression for hydrophobic proteins (*39*−*41*) because the MBP portion is water-soluble ($M_w \sim 40$ kDa) (*42*). Thus, we tried the pMal-c2 vector to obtain our polypeptides as an MBP-fusion protein. To prevent the influence of the unnecessary ISEF on our experiments, we modified the vector so as to possess an RG spacer between MBP and the objective hydrophobic polypeptide. This simple spacer allows enzymatic cleavage of the fusion protein between R and G by the common protease, trypsin. The designed polypeptides themselves have no cleavable site for trypsin. The trypsin does not cleave the C-terminal region of the polypeptides containing R, which is adjacent to P, because P forces the polypeptide chain to bend so as to be insensitive to hydrolysis by the trypsin.

Using the modified vector, the designed fusion proteins were successfully overexpressed (∼6 mg/1 L of culture) as described below. In Figure 2, the SDS−PAGE of the purified fusion proteins by affinity chromatography (MBP-**1**, lane 2; MBP-**2**, lane 5; and MBP-**4**, lane 8) are shown. For MBP-**1** lacking cysteine, a clear band was observed at the molecular weight of ca. 44 kDa (i.e., 40 kDa (MBP) + 3.7 kDa (**1**) = ∼44 kDa). Hydrolysis by trypsin gave the free MBP portion at the expected molecular mass (lane 3). The detached polypeptide, **1**, is invisible in the electrophoresis. Instead, RP-HPLC analysis clearly indicated that the hydrolysis process had been measured (Figure 3a). The peak of MBP-**1** at 10.0 min (solid line) completely vanishes and that of the

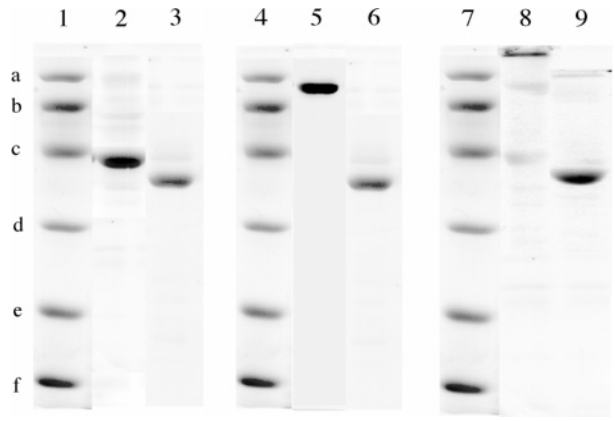

FIGURE 2: SDS−PAGEs of fusion proteins and their hydrolyzed mixtures. Lanes 1, 4, and 7 represent marker proteins (a, 97.4 kDa; b, 66.2 kDa; c, 45.0 kDa; d, 31.0 kDa; e, 21.5 kDa, and f, 14.4 kDa). Lanes 2, 5, 8 represent affinity-chromatographed fusion proteins, MBP-**1**, $(\text{MBP-}\mathbf{2})_2$, and $(\text{MBP-}\mathbf{4})_n$, respectively, and the corresponding trypsin-treated mixtures are shown in lanes 3, 6, and 9.

hydrolyzed product, **1**, appears at 14.9 min (dashed line, indicated by arrow). For MBP-**2** bearing a cysteine at the C-terminus, the affinity-chromatographed product shows an electrophoresis band at the doubled mass of ~88 kDa (lane 5 in Figure 2). After hydrolysis with trypsin, the band corresponding to the free MBP (40 kDa) was observed (lane 6 in Figure 2). The HPLC profile of the affinity-chromatographed MBP-**2** is shown in Figure 3b (solid line): the product was eluted at 11.5 min. By addition of an excess amount of 2-mercaptoethanol, the peak is shifted to 10.4 min (dashed line), which is comparable to that of the monomeric MBP-**1**. These observations clearly indicate that the affinity-chromatographed MBP-**2** is predominantly a dimerized form, $(\text{MBP-}\mathbf{2})_2$, via disulfide linkage. Treatment with trypsin of $(\text{MBP-}\mathbf{2})_2$ should provide the dimerized form, $(\mathbf{2})_2$. This trypsin-treated sample was subjected to RP-HPLC, showing a peak at 17.5 min (solid line in Figure 3c). By addition of an excess amount of 2-mercaptoethanol to this solution, the peak is shifted to 15.0 min (dashed line in Figure 3c). The latter peak was assigned to monomeric form, **2**. The product can be purified by the RP-HPLC as shown in Figure 3d (rt = 15.0 min). Although the chromatogram exhibits the single and sharp peak, the yield is very low (~1%), on the basis of the amount of the fusion protein formed. This is possibly due to the highly hydrophobic property of the polypeptide. For MBP-**3** bearing cysteine on the N-terminal region, the dimerization of MBP-**3** to form $(\text{MBP-}\mathbf{3})_2$ was observed as well. The retention times of MBP-**3** and $(\text{MBP-}\mathbf{3})_2$ were 10.1 and 11.7 min, respectively. The enzymatic cleavage was also successful giving the dimeric form $(\mathbf{3})_2$ (rt = 17.3 min) as well as the reduced form **3** (rt = 15.1 min).

Unlike MBP-**2** and MBP-**3** having cysteine either on the C- or N-terminal region, the SDS−PAGE of MBP-**4** bearing cysteine on both termini shows a high molecular weight product (lane 8), suggesting that the affinity-chromatographed product of MBP-**4** forms an oligomer, $(\text{MBP-}\mathbf{4})_n$, via multi-cross-linking of the cysteine residues. Despite the multi-cross-linkage, trypsin treatment successfully gives the free MBP (lane 9), indicating that the trypsin-treated product is obtained as oligomeric form, $(\mathbf{4})_n$. The product $(\mathbf{4})_n$ is easily reduced

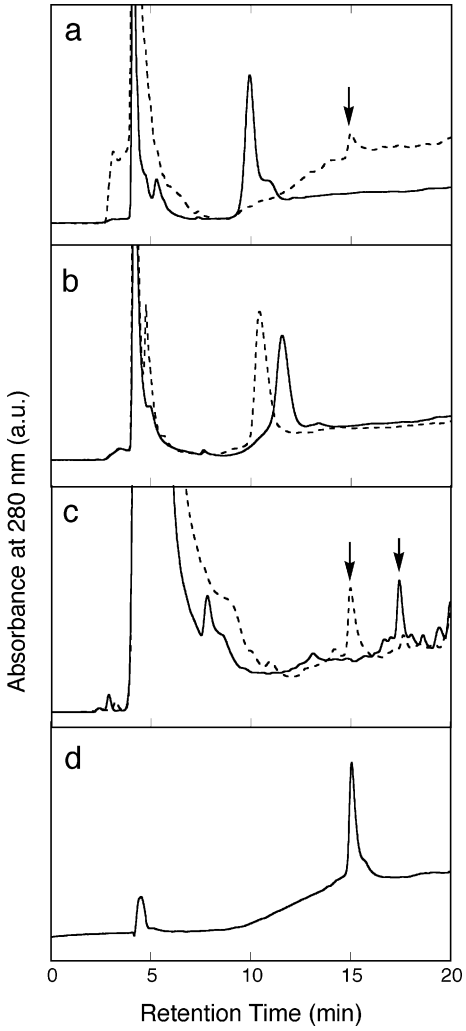

FIGURE 3: Reverse-phase (RP-)HPLC profiles of the fusion proteins and the hydrolyzed polypeptides. (a): MBP-**1** (solid line, rt = 10.0 min) and **1** (dashed line, rt = 14.9 min indicated by arrow); (b): $(\text{MBP-}\mathbf{2})_2$, (solid line, rt = 11.5 min) and its reduced form MBP-**2** (dashed line, rt = 10.4 min); (c) hydrolyzed polypeptide $(\mathbf{2})_2$ (solid line, rt = 17.5 min indicated by arrow) and its reduced form, **2**, (dashed line, rt = 15.0 min indicated by arrow); (d) the polypeptide **2** purified by preparative RP-HPLC (rt = 15.0 min).

by 2-mercaptoethanol to form the monomer, **4**, whose retention time, 15.1 min, is consistent with those of other monomeric polypeptides, **1**−**3**.

Assemblies of Pigment/Polypeptides with or without MBP Portion. Figure 4a and b shows the near-infrared (NIR) absorption and CD spectra of the assembled complex of [Zn]-BChl *a* with either MBP-**1** or **1** in an OG micellar solution at 4 °C. Free [Zn]-BChl *a* in an OG micellar solution has an absorption band (Qy) at 770 nm. In the presence of the MBP-**1** and **1**, red-shifted Qy bands are observed at 814 and 815 nm, respectively (Figure 4a). Under these conditions, asymmetrically split CD signals consisting of a major negative and of a minor positive band are also observed (Figure 4b). These spectra are characteristic of a subunit-type complex as previously reported for the subunit complex of BChl *a* or [Zn]-BChl *a* with LH1β isolated from *Rb. sphaeroides* (*16*, *18*, *25*, *26*). Regardless of the enzymatic cleavage of the MBP portion, the spectra are almost identical (solid and dashed line). The other fusion proteins and the detached polypeptides also form subunit-type complexes with

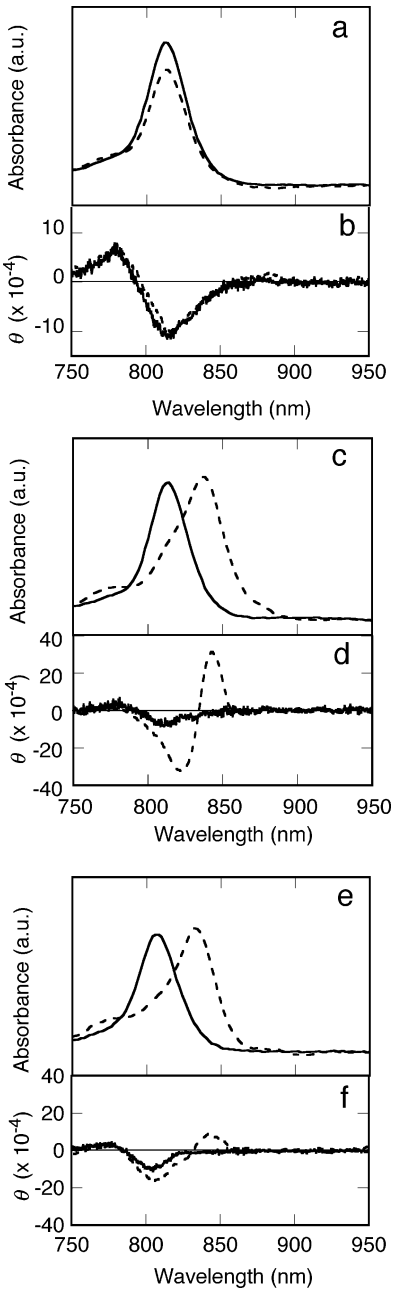

FIGURE 4: Absorption (**a**, **c**, **e**) and CD (**b**, **d**, **f**) spectra of [Zn]-BChl *a* reconstituted with various types of fusion proteins or polypeptides. (**a**, **b**), MBP-**1** (solid line) and **1** (dashed line); (**c**, **d**), MBP-**2** (solid line) and **2** (dashed line) in the presence of 2-mercaptoethanol; (**e**, **f**), (MBP-**2**)$_2$ (solid line) and (**2**)$_2$ (dashed line). All spectra were obtained at 4 °C after storage of the samples at 4 °C for 3 days.

[Zn]-BChl *a* at 25 °C. The complete set of spectral data from these assemblies has been summarized in Table 1.

Monomeric types of fusion proteins and polypeptides bearing cysteines were prepared from the corresponding oxidized forms by reduction of 2-mercaptoethanol for the reconstitution experiments. By cooling to 4 °C, the enzymatically detached polypeptide **2** assembled with [Zn]-BChl *a* shows a prominent red-shifted Qy band at 836 nm, as shown in Figure 4c (dashed line) and Table 1 (entry 5). The CD spectrum of this assembly also changes to give a split signal, which is characteristic of an LH1-type complex (*26*) where the BChl *a* pigments align in an excitonically coupled way. In contrast, the absorption and CD spectra of the assembly of MBP-**2** with [Zn]-BChl *a* show the features characteristic of a subunit-type complex (solid line in Figure 4c and d, and entry 3 in Table 1). These observations strongly suggest that **2** possesses a propensity to form a pigment/polypeptide assembly in which the pigments alignment resembles LH1-type complex. The MBP portion is large enough to sterically prevent the formation of such an LH1-type complex, restricting the assembly to that of the subunit type. Complexation of the **4** with [Zn]-BChl *a* produces a similar product to that obtained with **2**: the cleavage of MBP shifts the Qy band from 813 nm (MBP-**4**; entry 11) to 836 nm (**4**; entry 13) and alters the CD signals as well. Such an effect of MBP cleavage on the complexation for **3** is insignificant compared with the **2** and **4** (entries 7 and 9).

As a control, the results of the reconstitution assay with the native polypeptides, that is, LH1α + LH1β and LH1β alone, and the chemically synthesized LH1β with [Zn]-BChl *a* are also listed in Table 1 (entries 15−17). The native-type combination, LH1α + LH1β, shows a progressive assembly from the subunit-type to the LH1-type complex on cooling to 4 °C. The single polypeptide, LH1β native or synthetic, when added to [Zn]-BChl *a*, forms a subunit-type complex at 25 °C. The synthetic LH1β polypeptide alone further assembles to an LH1-type at 4 °C, judged from its Qy absorption maximum and the characteristic split of the CD signal (*25*).

Figure 5a−c shows the fluorescence spectra together with the absorption spectra of the complexes obtained with LH1β, MBP-**2**, and **2** and [Zn]-BChl *a* at various excitation wavelengths in the Qy band region. The complex, LH1β/[Zn]-BChl *a*, exhibits well-characterized emission from subunit complex: the λ_{max} of emission band at 824 nm with ∼10 nm of Stokes shift that is independent of the excitation wavelength. The relative fluorescence intensity is obviously increased with the excitation wavelength in the range of 770−800 nm (Figure 5a). Similar emission spectra whose λ_{max} is independent from excitation wavelength are also observed for the MBP-**2**/[Zn]-BChl *a* complex (Figure 5b). This is further explicit evidence that the complex is of the subunit type. For **2**/[Zn]-BChl *a* complex (Figure 5c), the emission spectrum (λ_{em} = 853 nm) with ∼23 nm of Stokes shift is observed when excited at 830 nm near the absorption maximum. The fluorescence is characteristic of the LH1-type complex; this confirms that **2** forms an LH1-type complex with [Zn]-BChl *a*. The emission profiles of λ_{em} = 789 and 820 nm are broad and heterogeneous. This indicates that monomeric and subunit-type complexes are also present.

Effect of Disulfide Linkage between Polypeptides on the Complexation with the Pigment. As described above, affinity-chromatographed products bearing cysteines, MBP-**2**, -**3**, and -**4** are obtained as oxidized forms, (MBP-**2**)$_2$, (MBP-**3**)$_2$, and (MBP-**4**)$_n$, respectively. The corresponding detached polypeptides also contain disulfide links, (**2**)$_2$, (**3**)$_2$, and (**4**)$_n$. The assembly properties of these dimeric and oligomeric proteins (polypeptides) were also examined. Figure 4e and 4f shows the NIR absorption and CD spectra for the complexes of [Zn]-BChl *a* with (MBP-**2**)$_2$ and (**2**)$_2$ at 4 °C. The Qy bands appear at 807 and 832 nm for complexes of (MBP-**2**)$_2$ and (**2**)$_2$, respectively. The CD spectra (Figure 4f) showed a negative peak at 803 nm for (MBP-**2**)$_2$ and split peaks at 842 and 806 nm for (**2**)$_2$. From these spectral features, it is reasonable to suggest that the complexes of (MBP-**2**)$_2$ and

Table 1: NIR Absorption and CD Spectral Data of [Zn]-BChl *a* Assembled with Various Types of Fusion Proteins and Hydrophobic Polypeptides

		Qy absorption bands/nm		CD maxima/nm (10^{-4} β)
entry	polypeptide	25 °C	4 °C	4 °C
1	MBP-**1**	813	814	814 (−10)
2	**1**[a]	812	815	815(−10)
3	MBP-**2**	810	813	812 (−10)
4	(MBP-**2**)$_2$	806	807	803 (−10)
5	**2**[a]	812	836	842 (32), 822 (−32)
6	(**2**)$_2$[a]	806	832	842 (9), 806 (−16)
7	MBP-**3**	812	814	810 (−10)
8	(MBP-**3**)$_2$	812	812	804 (−10)
9	**3**[a]	812	818	844 (4), 818 (−15)
10	(**3**)$_2$[a]	814	816	810 (−8)
11	MBP-**4**	811	813	810 (−12)
12	(MBP-**4**)$_n$	809	809	806 (−9)
13	**4**[a]	816	836	844 (20), 822 (−25)
14	(**4**)$_n$[a]	808	815	843 (5), 810 (−10)
15	LH1α + LH1β[b]	812	859	867 (8), 832 (−6)
16	LH1β[b]	814	817	822 (−6)
17	synthetic LH1β[c]	810	834	838 (33), 817 (−36)

[a] The polypeptide was subjected to the reconstitution assay as a solution after the cleavage by trypsin. [b] LH1α and LH1β polypeptides were isolated from *Rhodobacter sphaeroides.* Spectral data were cited from ref (*25*). [c] Chemically synthesized polypeptide (see Figure 1 and ref (*25*)).

(**2**)$_2$ with [Zn]-BChl *a* are subunit- and LH1-types, respectively. With the other dimeric systems, (MBP-**3**)$_2$ and (**3**)$_2$ (entries 8 and 10), subunit-type complex formation was observed in the manner similar to (MBP-**2**)$_2$ and (**2**)$_2$.

The randomly cross-linked protein, (MBP-**4**)$_n$, was also able to assemble with [Zn]-BChl *a*, and its Qy absorption band and its CD profile indicated that its assembly was of the subunit type (entry 12). Assembly of (**4**)$_n$ with [Zn]-BChl *a* also produces a subunit-type complex (entry 14). Although the CD split pattern resembles that of LH1 type, the split pattern is not symmetrical (the negative peak at 810 nm is larger than the positive one at 843 nm). Thus, the pigment alignment of the complex of (**4**)$_n$ is predominantly a subunit-type one, possibly including the LH1-type one as a minor component in the complex. By addition of 2-mercaptoethanol in the solution of the assembly of (**4**)$_n$ with [Zn]-BChl *a*, the Qy band shifts to ∼836 nm corresponding to an LH1-type complex. This observation suggests that the transformation of the pigment array results from the cleavage of random cross-linkage of the polypeptide (**4**)$_n$ by the reduction by 2-mercaptoethanol.

Assembling Property of BChl a. A [Zn]-BChl *a* is a naturally occurring photosynthetic pigment found in *Acidiphilium rubrum* (*43*); meanwhile, a BChl *a* is one of the most common pigments of bacterial photosynthetic systems. The [Zn]-BChl *a* possesses greater chemical stability and its coordination ability is also considerably higher than that of magnesium in BChl *a* (*34*). Figure 6 shows NIR absorption spectra resulting from the assembly of **3** with either BChl *a* (solid line) or [Zn]-BChl *a* (dashed line). As mentioned above, when **3** was assembled with [Zn]-BChl *a*, red-shifted Qy band is observed at 818 nm (dashed line in Figure 6) with a small shoulder band at 770 nm, which comes from monomeric [Zn]-BChl *a* pigment in the OG solution. Parallel experiments with BChl *a* produce a product which shows a much larger peak at 776 nm as well as one at 824 nm. The CD spectrum of the product (solid line: inset in Figure 6) shows a major negative band maximum at 823 nm and a minor positive band characteristic of a subunit-type complex. The prominent monomeric peak at 776 nm, however, indicates that the formation of subunit-type com-

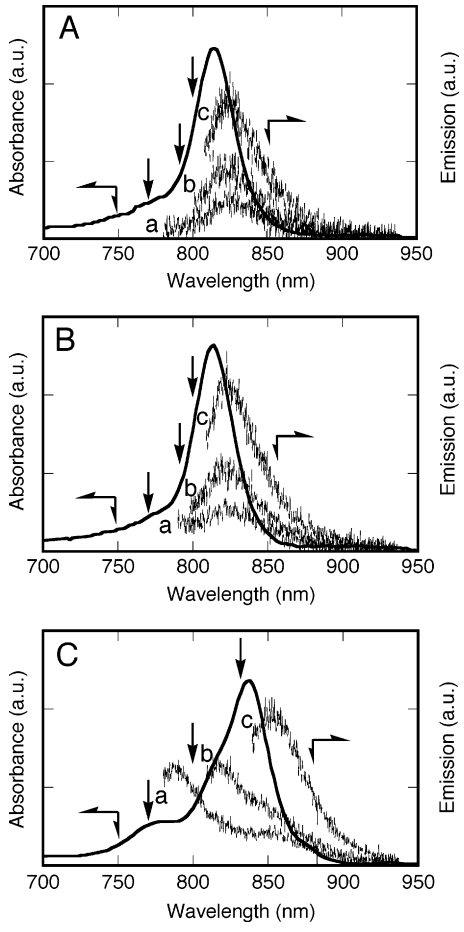

FIGURE 5: Absorption (smooth solid lines) and fluorescence (jagged lines) spectra of [Zn]-BChl *a* assembled with various polypeptides: β polypeptide derived from *Rb. sphaeroides*, (A); MBP-**2**, (B); and **2**, (C). Vertical arrows indicate the fluorescence excitation wavelengths: 770, 790, and 800 nm for A and B; 770, 800, and 830 nm for C. Fluorescence spectra obtained by these excitation wavelengths are denoted by a, b, and c, respectively. These spectra were obtained at 4 °C after storage of the samples at 4 °C for 3 days. Exposure time of CCD detector was 10 s. Relative fluorescence intensity for each sample is normalized by automatic calibration by using an equipped photodiode detector and operating software (WinSpec/32, Roper Scientific co.).

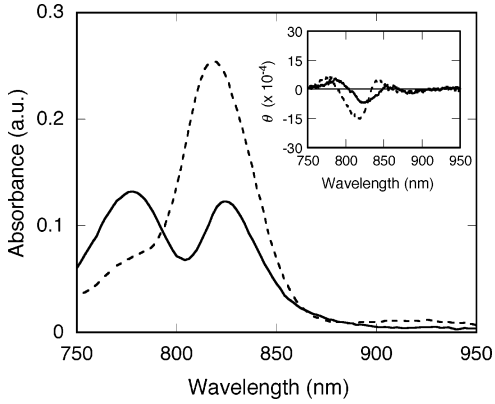

FIGURE 6: Absorption spectra of reconstituted BChl *a* (solid line) and [Zn]-BChl *a* (dashed line) with **3** in 0.78 wt % OG solution at 4 °C. Inset: CD spectra of the corresponding samples: BChl *a* (solid line) and [Zn]-BChl *a* (dashed line).

plex is incomplete because of the lower affinity of BChl *a* for the polypeptide than that of [Zn]-BChl *a*. When BChl *a* is assembled with other polypeptides, that is, **1**, **2**, and **4**, the two peaks at 776 and 822 nm appear in the similar way to the **3**, regardless of the presence of cross-links or the presence of the MBP portion.

Incorporation and Assembling of the Polypeptide/Pigment Complex in a Lipid Bilayer. The subunit-type complex, (MBP-**2**)$_2$/[Zn]-BChl *a*, was incorporated into a lipid bilayer consisting of DOPG via dialysis of the reconstitute comicellar solution. In the bilayer phase, the Qy band observed at 806 nm is indicative of the subunit-type complex. By treatment with trypsin, removal of MBP portion was confirmed by SDS−PAGE. After the solution stood for a few days at 4 °C, the Qy band shifted to ∼830 nm. This red-shift of the Qy absorption suggests that in the lipid bilayer phase the subunit type of (MBP-**2**)$_2$/[Zn]-BChl *a* reassembles to LH1-type complex of (**2**)$_2$/[Zn]-BChl *a* via trypsin treatment.

DISCUSSION

Subunit-Type Complex Formation of the MBP-Fusion Proteins with Pigments. The reconstitution methodology developed by Loach's group has provided important structural information about not only a core LH1 complex but also a subunit complex which has the composition α_1/β_1/2BChl *a* as a minimal structural unit for the core complex (*13*−*18*). The core LH1 and the subunit complexes possess their own characteristic absorption (Qy) band and CD split patterns; therefore, such complex formation is distinguishable. The LH1β of *Rb. sphaeroides* forms subunit-type complex with pigment [Zn]-BChl *a* or BChl *a*, showing that the Qy band was red-shifted to 817 or 820 nm, respectively, as described previously (see Table 1) (*18*, *24*−*26*). The minimal number of amino acids required for subunit formation has been reported to be 31 from the C-terminal of the *Rb. sphaeroides* polypeptide (*16*). The investigated fusion proteins, whose amino acid sequence of the hydrophobic portions fulfill the requirement, formed the subunit-type complex on the basis of the spectroscopic evidences (absorption, CD, and fluorescence spectra). Therefore, it is tentatively interpreted that it would be reasonable for the subunit formation of the fusion proteins along the same line with that of the native LH1β of *Rb. sphaeroides*. Further, the wavelength of the observed Qy bands, ∼836 nm, of these assemblies, **2** or **4**, with [Zn]-BChl *a* showed good agreement with that of the chemically synthesized LH1β, 834 nm (entry 17) (*25*). This moderate red-shifted value, ∼836 nm, was indicative of the formation of LH1 complex.

The MBP portion (40 kDa) is 10 times as large as the hydrophobic polypeptides. An X-ray crystallographic structure of MBP itself is ellipsoidal with dimensions of 30 × 40 × 65 Å (*42*), while the polypeptide part can be assumed to be ca. 40 Å helix on the basis of the hydrophobic transmembrane region. As previously reported, the LH1β of *Rb. sphaeroides* forms a subunit-type complex with the pigments BChl *a* and [Zn]-BChl *a* (*16*, *21*−*25*). The LH1β polypeptide is comprised of two α-helical domains, which are divided by hinge part, position −12(G) ∼ −10(W) (Figure 1) (*19*). Despite the presence of a large part of α-helical domain in the N-terminal region, the LH1β forms subunit-type complex with BChl *a*. The present hydrophobic polypeptides involve the required amino acids as described above (*16*). This hydrophobic sequence is so essential that such fusion proteins form the subunit-type complexes. In Figure 7, the assembling experiment in this study is schematically illustrated by how proteins and pigments assemble via various processes starting from (MBP-**2**)$_2$ as a representative sample.

Regardless the presence or absence of the cross-links via disulfide bonds, all of the fusion proteins form subunit-type complexes. However, the Qy bands of these assemblies with [Zn]-BChl *a* are blue-shifted by 6 nm in the presence of the cross-links (entry 3 vs 4). When the subunit complex of (MBP-**2**)$_2$, for example, is reduced by an excess amount of 2-mercaptoethanol, the Qy band red-shifts from 807 to 813 nm at 4 °C. This suggests that the disulfide linkage has a steric influence on the pigment alignment. Alternatively, the reduced form, free from the steric restriction of the linkage, might prefer to assemble in a similar way to native LH1β/[Zn]-BChl *a* combination. Such change in 6 nm of the Qy band may be small but the pigment alignment is "finely tuned" by redox (cross-link/cleavage) state of the terminal cysteine. The position of the essential amino acid, H (position 0), which coordinates to the central metal of the [Zn]-BChl *a*, is vicinal toward the C-terminus rather than the opposite side. The C-terminal cross-linked fusion protein, (MBP-**2**)$_2$, exhibits perturbation in its pigment alignment (by 6 nm of blue-shift) compared with the monomeric form, MBP-**2**. On the other hand, the N-terminal cross-linked (MBP-**3**)$_2$, which possesses more conformational freedom for the pigment binding and alignment than (MBP-**2**)$_2$, shows less difference in its Qy band (2 nm) compared with its monomeric form, MBP-**3** (entry 7 vs 8).

LH1-Type Complexation of MBP-Free Polypeptide. Removal of the MBP portion allows polypeptides **2** and **4** to assemble with [Zn]-BChl *a* to form an LH1-type complex. This suggests that liberation from steric hamper allows **2** and **4** to progressively assemble with [Zn]-BChl *a*. When (MBP-**2**)$_2$/[Zn]-BChl *a* is directly treated with trypsin after dialysis (to remove OG), the subunit assembly spontaneously aggregates further to form the LH1 type complex. The wavelength of the observed Qy bands, ∼836 nm, of the assembly shows good agreement with the complex formed with the chemically synthesized LH1β, 834 nm (entry 17) (*25*).

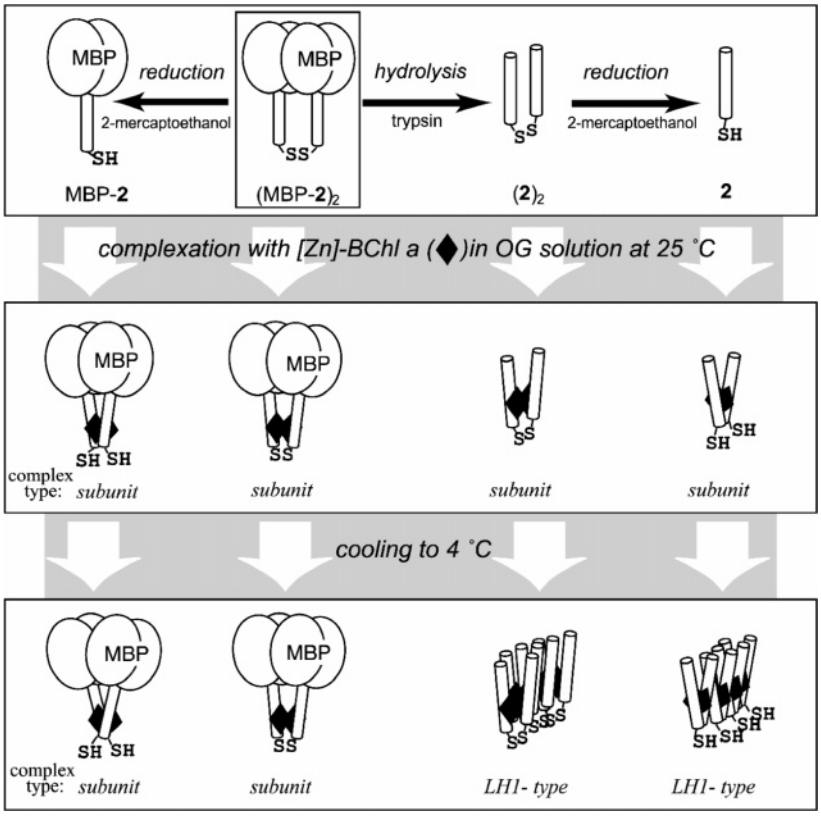

FIGURE 7: Schematic illustration of the assemblies of [Zn]-BChl *a* with the MBP-**2**, (MBP-**2**)$_2$, **2**, and (**2**)$_2$. Ellipsoidal, cylindrical, and black-rhombic portions represent MBP, polypeptide **2**, and [Zn]-BChl *a*, respectively. The illustrated structure of the fusion proteins, MBP-**2**, (MBP-**2**)$_2$, are putative on the basis of the crystal structure of maltose-binding protein (ref 42). The C-terminus of the protein is placed on the outer sphere between two domains. Supposing the structure of the expressed MBP is similar to the reported structure, the polypeptide should attach to the place of the C-terminus as depicted in this figure.

In previous experiments with reconstituted complexes, we have observed a relation between the wavelength of Qy band and the complex size estimated by SAXS and DLS (*24*, *34*). The estimated sizes correlate well with the extent of red-shifted Qy band. The moderate red-shifted value, ~ 836 nm, is indicative of the formation of LH1-type complex.

The presence or absence of the disulfide linkage shifts the Qy absorption band for **2**/(**2**)$_2$ (entry 5 vs 6) by 4 nm at 4 °C. The most dramatic change (21-nm difference in the Qy band) is observed for **4** and (**4**)$_n$ (entry 13 vs 14): here, random cross-linking in the latter strongly inhibits the LH1-type formation. This result clearly indicates that the orientation of the polypeptide is an essential factor for the LH1-type assembly. When an excess amount of 2-mercaptoethanol is added in the solution of (**4**)$_n$/[Zn]-BChl *a*, the Qy band and CD signal are transformed into those of an LH1-type complex identical to the **4**/[Zn]-BChl *a* complex. The observed reassembly process from (**4**)$_n$/[Zn]-BChl *a* (subunit-type) to **4**/[Zn]-BChl *a* (LH1-type) further supports the importance of the orientation of the polypeptide.

Transformation of the Subunit-Type to LH1-Type Complex in a Lipid Bilayer. The unexpected result of subunit-type complex formation of the MBP-fusion proteins prompted us to examine the assembling property in a lipid bilayer. In a preliminary study, we incorporated the subunit-type complex, (MBP-**2**)$_2$/[Zn]-BChl *a*, into a lipid bilayer consisting of DOPG. The assembling process is depicted in Figure 8. After dialysis, the observed Qy band at 806 nm indicates subunit-type complexation (state b). By treatment with trypsin, the subunit assembly of (MBP-**2**)$_2$/[Zn]-BChl *a* can be hydrolyzed to release MBP portion. By cooling at 4 °C, the resulting complex exhibits the red-shifted Qy absorption band indicative of LH1-type complex (state d). This assembling process should involve subunit-type complex (state c) before further assembled state (d), because it takes a few days to reach state d at 4 °C. This observation clearly demonstrates the progressive self-assembling event of hydrophobic polypeptide to form LH1-type complex in the membrane phase.

Such assembling process in the lipid bilayer involves important phenomena in biological aspect: insertion of membrane protein into a cell membrane, enzymatic protein splicing (cleavage of signal polypeptide), followed by self-assembling process to form a membrane protein complex (LH1 complex in this case). If one would regard the MBP portion as "an anchor" or "a buoy" to regulate the orientation of the polypeptide for asymmetrical photosynthetic membranes, the present observation using the MBP fusion proteins with model polypeptides is of interest. In this regard, the present system is a unique and potentially useful tool for investigating self-assembling processes of membrane proteins. In addition, the common pigment, BChl *a*, is also applicable to such an experimental system. This can be expected to provide more general aspects of such polypeptide/pigment assembly properties in a lipid bilayer.

CONCLUSIONS

We have described the successful expression of the bacterial LH1 polypeptides as MBP-fusion proteins by using *E. coli* expression system. To the best of our knowledge,

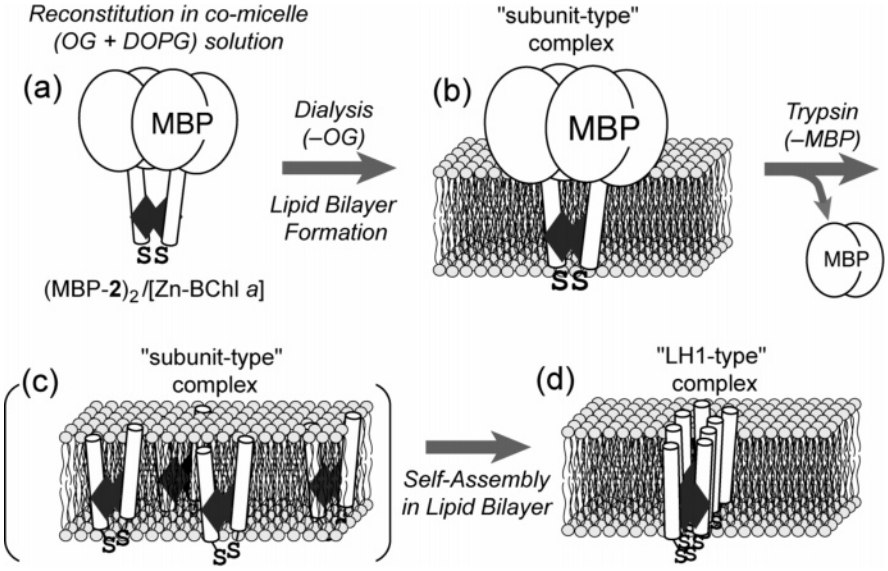

FIGURE 8: Schematic illustration of transformation of subunit-type complex, (MBP-**2**)$_2$/[Zn]-BChl *a*, (states a and b) into LH1-type complex, (**2**)$_2$/[Zn]-BChl *a*, (state d) in a lipid bilayer (DOPG) via trypsin-treatment process. The ratio of the components, DOPG/(MBP-**2**)$_2$/[Zn]-BChl *a*, is 100/4/1. The subunit-type complex, (MBP-**2**)$_2$/[Zn]-BChl *a*, was reconstituted in OG and DOPG comicelle solution (a), followed by dialysis with phosphate buffer (50 mM, pH 7.0) to form a lipid bilayer (b). The resulting solution was treated with trypsin at 37 °C to cleave the MBP portion. The digested assemblies (c) further associate each other to form "LH1-type" complex (d). The transformation of the complex type was judged by the Qy absorption band.

this is the first report describing the expression and the assembling properties of the LH-like polypeptides produced in this way. It should be noted that (i) a series of MBP-fusion proteins assemble with [Zn]-BChl *a* to form subunit-type complexes despite the presence of the large MBP portion and (ii) the disulfide linkage/cleavage finely perturbs the pigment alignment. Also, (iii) the observation that all the cleaved polypeptides formed subunit-type complex at 25 °C, regardless of the redox state (cysteine/cystine) and its position, indicates that the disulfide linkage is not crucial for the formation of subunit assembly but affects the pigment alignment. Unlike the assembly of (**2**)$_2$ with [Zn]-BChl *a*, which forms LH1-type complex at 4 °C, the randomly cross-linked (**4**)$_n$ does not form the complex. This suggests that the orientation of the polypeptide is an essential factor in the polypeptide/pigment assembly process. The approach described in this report provides useful information on how to investigate the pigment alignment in the light-harvesting complex and how this can be controlled. Our interest is now moving to study the reconstitution of these assemblies in lipid bilayers. Efforts aimed at exploring such an interest are now in progress.

ACKNOWLEDGMENT

Authors thank professors Richard J. Cogdell (University of Glasgow, U.K.) and Paul A. Loach (Northwestern University) for critical comments and discussion.

REFERENCES

1. Ke, B. (2001) in *Photosynthesis, Photobiochemistry and photobiophysics*, Advances in Photosynthesis, Vol. 10 (Govindjee, Series Ed.) Kluwer Academic Publishers, Dordrecht, The Netherlands.
2. Blankenship, R. E. (2002) *Molecular Mechanisms of Photosynthesis*, Blackwell Science Ltd., Oxford.
3. Robert, B. Cogdell, R. J., and van Grondelle, R. (2003) Chapter 5 in *Light-harvesting Antennas in Photosynthesis* (Green, B. R., and Parson W. W. Eds.) Advances in Photosynthesis and Respiration, Vol. 13 (Govindee, Series Ed.) Kluwer Academic Publishers, Dordrecht, The Netherlands.
4. McDermott, G., Prince, S. M., Freer, A. A., Hawthornthwaite-Lawless, A. M., Papiz, M. Z., Cogdell, R. J., and Isaacs, N. W. (1995) Crystal structure of an integral membrane light-harvesting complex from photosynthetic bacteria, *Nature 374*, 517−521.
5. Deisenhofer, J., Epp, O., Sinning, I., and Michel, H. (1995) Crystallographic refinement at 2.3 Å resolution and refined model of the photosynthetic reaction center from *Rhodopseudomonas viridis*, *J. Mol. Biol. 246*, 429−457.
6. Katona, G., Andréasson, U., Landau, E. M., Andréasson, L.-E., and Neutze, R. (2003) Lipidic cubic phase crystal structure of the photosynthetic reaction centre from *Rhodobacter sphaeroides* at 2.35 Å resolution, *J. Mol. Biol. 331*, 681−692.
7. Roszak, A. W., Howard, T. D., Southall, J., Gardiner, A. T., Law, C. J., Isaacs, N. W., and Cogdell, R. J. (2003) Crystal structure of the RC-LH1 core complex from *Rhodopseudomonas palustris*, *Science 302*, 1969−1972.
8. Karrasch, S., Bullough, P. A., and Ghosh. R. (1995) The 8.5 Å projection map of the light-harvesting complex I from *Rhodospirillum rubrum* reveals a ring composed of 16 subunits, *EMBO J. 14*, 631−638.
9. Fotiadis, D., Qian, P., Philippsen, A., Bullough, P. A., Engel, A., and Hunter, C. N. (2004) Structural analysis of the reaction center light-harvesting complex I photosynthetic core complex of Rhodospirillum rubrum using atomic force microscopy, *J. Biol. Chem. 279*, 2063−2068.
10. Bahatyrova, S., Frese, R. N., van der Werf, K. O., Otto, C., Hunter, C. N., and Olsen, J. D. (2004) Flexibility and size heterogeneity of the LH1 light harvesting complex revealed by atomic force microscopy, *J. Biol. Chem. 279*, 21327−21333.
11. Bahatyrova, S., Frese, R. N., Siebert, C. A., Olsen, J. D., van der Werf, K. O., van Grondelle, R., Niederman, R. A., Bullough, P. A., Otto, C., and Hunter, C. N. (2004) The native architecture of a photosynthetic membrane, *Nature 430*, 1058−1062.
12. Scheuring, S., Sturgis, J. N., Prima, V., Bernadac, A., Lévy, D., and Jean-Louis Rigaud, J.-L. (2004) Watching the photosynthetic apparatus in native membranes, *Proc. Natl. Acad. Sci. U.S.A. 101*, 11293−11297.
13. Miller, J. F., Hinchigeri, S. B., Parks-Loach, P. S., Callahan, P. M., Sprinkle, J. R., Riccobono, J. R., and Loach, P. A. (1987) Isolation and characterization of a subunit form of the light-harvesting complex of *Rhodospirillum rubrum*, *Biochemistry 26*, 5055−5061.
14. Parkes-Loach, P. S., and Loach, P. A. (1995) Structure-function relationships in core light-harvesting complex (LH1) as determined by characterization of the structural subunit and by reconstitution

experiments, in *Anoxygenic Photosynthetic Bacteria* (Blankenship, R. E., Madigan, T. M., and Bauer, C. D., Eds.) Chapter 21, pp 437−471, Kluwer Academic Publishers, Dordrecht, The Netherlands.
15. Parkes-Loach, P. S., Majeed, A. P., Law, C. J., and Loach, P. A. (2004) Interactions stabilizing the structure of the core light-harvesting complex (LH1) of photosynthetic bacteria and its subunit (B820), *Biochemistry 43*, 7003−7016.
16. Meadows, K. A., Parkes-Loach, P. S., Kehoe, J. W., and Loach, P. A. (1998) Reconstitution of core light-harvesting complexes of photosynthetic bacteria using chemically synthesized polypeptides. 1. Minimal requirements for subunit formation, *Biochemistry 37*, 3411−3417.
17. Todd, J. B., Recchia, P. A., Parkes-Loach, P. S., Olsen, J. D., Fowler, G. J. S., McGlynn, P., Hunter, C. N., and Loach, P. A. (1999) Minimal requirements of *in vitro* reconstitution of the structural subunit of light-harvesting complexes of photosynthetic bacteria, *Photosynth. Res. 62*, 85−98.
18. Meadows, K. A., Iida, K., Tsuda, K., Recchia, P. A., Heler, B. A., Antonio, B., Nango, M., and Loach, P. A. (1995) Enzymatic and chemical cleavage of the core light-harvesting polypeptides of photosynthetic bacteria: determination of the minimal polypeptide size and structure required for subunit and light-harvesting complex formation, *Biochemistry 34*, 1559−1574.
19. Conroy, M. J., Westerhuis, W. H. J., Parkes-Loach, P. S., Loach, P. A., Hunter, C. N., and Williamson, M. P. (2000) The solution structure of *Rhodobacter sphaeroides* LH1β reveals two helical domains separated by a more flexible region: Structural consequences for the LH1 complex, *J. Mol. Bol. 298*, 83−94.
20. Wang, Z. Y., Muraoka, Y., Nagao, M., Shibayama, M., Kobayashi, M., and Nozawa, T. (2003) Detemination of the B820 subunit size of a bacterial core light-harvesting complex by small-angle neutron scattering, *Biochemistry 42*, 11555−11560.
21. Sorgen, P. L., Cahill, S., M., Krueger-Koplin, R. D., Krueger-Koplin, S. T., Schenck, C. C., and Girvin, M. E. (2002) Structure of the *Rhodobacter sphaeroides* light-harvesting 1β subunit in detergent micelles, *Biochemistry 41*, 31−41.
22. Wang, Z. Y., Muraoka, Y., Shimonaga, M., Kobayashi, M., and Nozawa, T. (2002) Selective detection and assignment of the solution NMR signals of bacteriochlorophyll *a* in a reconstituted subunit of a light-harvesting complex, *J. Am. Chem. Soc. 124*, 1072−1078.
23. Davis, C. M., Parkes-Loach, P. S., Cook, C. K., Meadows, K. A., Bandilla, M., Scheer, H., and Loach, P. A. (1996) Comparison of the structural requirements for bacteriochlorophyll binding in the core light-harvesting complexes of *Rhodospirillum rubrum* and *Rhodobacter sphaeroides* using reconstitution methodology with bacteriochlorophyll analogues, *Biochemistry 35*, 3072−3084.
24. Nango, M. (2005) Molecular assembly of bacteriochlorophyll complexes using synthetic light-harvesting model polypeptides, in *Chlorophylls and Bacteriochlorophylls: Biochemistry, Biophysics and Biological Function* (Grimm, B., Porra, R. J., Rüdiger, W., and Scheer, H., Eds.) Chapter 28, Kluwer Academic Publishers, Dordrecht, The Netherlands, in press.
25. Kashiwada, A., Watanabe, H., Tanaka, T., and Nango, M. (2000) Molecular assembly of zinc bacteriochlorophyll a by synthetic hydrophobic 1α-helix polypeptide, *Chem. Lett.* 24−25.
26. Nango, M., Kashiwada, A., Watanabe, H., Yamada, S., Yamada, T., Ogawa, M., Tanaka, T., and Iida, K. (2002) Molecular assembly of bacteriochlorophyll *a* using light-harvesting model 1α-helix polypeptides and 2α-helix polypeptide with disulfide-linkage, *Chem. Lett.* 312−313.
27. Arluison, V., Seguin, J., Le Caer, J.-P., Sturgis, J. N., Robert, B. (2004) Hydrophobic pockets at the membrane interface: An original mechanism for membrane protein interactions, *Biochemistry 43*, 1276−1282.
28. Markvart, T. (2000) Light harvesting for quantum solar energy conversion, *Prog. Quantum Electon. 24*, 107−186.
29. Gust, D., Moore, T. A., and Moore, A. L. (2001) Mimicking photosynthetic solar energy transduction, *Acc. Chem. Res. 34*, 40−48.
30. Robertson, D. E., Farid, R. S., Moser, C. C., Urbauer, J. L., Mulholland, S. E., Pidikiti, R., Lear, J. D., Wand, A. J., DeGrado, W. F., and Dutton, P. L. (1994) Design and synthesis of multihaem proteins, *Nature 368*, 425−432.
31. Shifman, J. M., Gibney, B. R., Sharp, R. E., and Dutton, P. L. (2000) Heme redox potential control in *de novo* designed four-α-helix bundle proteins, *Biochemistry 39*, 14813−14821.
32. Hill, R. B., Raleigh, D. P., Lombardi, A., and DeGrado, W. F. (2000) De novo design of helical bundles as models for understanding protein folding and function, *Acc. Chem. Res. 33*, 745−754.
33. Razeghifard, M. R., and Wydzynski, T. (2003) Binding of Zn-chlorin to a synthetic four-helix bundle peptide through histidine ligation, *Biochemistry 42*, 1024−1030.
34. Nagata, M., Nango, M., Kashiwada, A., Yamada, S. Ito, S., Sawa, N., Ogawa, M., Iida, K., Kurono, Y., and Ohtsuka, T. (2003) Construction of photosynthetic antenna complex using light-harvesting polypeptide-α from photosynthetic bacteria, *R. rubrum* with zinc substituted Bacteriochlorophyll *a*, *Chem. Lett.* 216−217.
35. Hunter, C. N. (1995) Genetic Manipulation of the Antenna Complexes of Purple Bacteria, in *Anoxygenic Photosynthetic Bacteria* (Blankenship, R. E., Madigan, T. M., and Bauer, C. D., Eds.) Chapter 22, pp 473−501, Kluwer Academic Publishers, Dordrecht, The Netherlands.
36. Maina, C. V., Riggs, P. D., Grandea, A. G., III, Slatko, B. E., Moran, L. S., Tagliamonte, J. A., McReynolds, L. A., and Guan, C. D. (1988) An *Escherichia coli* vector to express and purify foreign proteins by fusion to and separation from maltose-binding protein, *Gene 74*, 365−373.
37. Yin, H. L., Iida, K., and Janmey, P. A. (1988) Identification of a polyphosphoinositide-modulated domain in gelsolin which binds to the sides of actin filaments, *J. Cell Biol. 106*, 805−812.
38. Loach, P. A., Parks-Loach, P. S., Davis, C. M., and Heller, B. A. (1994) Probing protein structure requirements for formation of the core light-harvesting complex of photosynthetic bacteria using hybrid reconstitution methodology, *Photosynth. Res. 40*, 231−245.
39. Fox, J. D., Routzahn, K. M., Bucher, M. H., and Waugh, D. S. (2003) Maltodextrin-binding proteins from diverse bacteria and archaea are potent solubility enhancers, *FEBS lett. 537*, 53−57.
40. Bach, H., Mazor, Y., Shaky, S., Shoham-Lev, A., Berdichevsky, Y., Gutnick, D. L., and Benhar, I. (2003) *Escherichia coli* maltose-binding protein as a molecular chaperone for recombinant intercellular cytoplasmic single-chain antibody, *J. Mol. Biol. 312*, 79−93.
41. Miroux B., and Walker, J. E. (1996) Over-production of proteins in *Escherichia coli*: Mutant hosts that allow synthesis of some membrane proteins and globular proteins at high levels, *J. Mol. Biol. 260*, 289−298.
42. Spurlino, J. C., Lu, G.-Y., and Quiocho, F. A. (1991) The 2.3-Å resolution structure of the maltose- or maltodextrin-binding protein, a primary receptor of bacterial active transport and chemotaxis, *J. Biol. Chem. 266*, 5202−5219.
43. Wakao, N., Yokoi, N., Isoyama, N., Hiraishi, A., Shimada, K., Kobayashi, M., Kise, H., Iwaki, M., Itoh, S., Takaichi, S., and Sakurai, Y. (1996) Discovery of Natural photosynthesis Zn-containing bacteriochlorophyll in an aerobic bacterium *Acidiphilium rubrum*, *Plant Cell Physiol. 37*, 889−893.

BI0478493